Free-volume microstructure of glycerol and its supercooled liquid-state dynamics

2001 J. Phys.: Condens. Matter 13 11473

(http://iopscience.iop.org/0953-8984/13/50/307)

INSTITUTE OF PHYSICS PUBLISHING JOURNAL OF PHYSICS: CONDENSED MATTER

J. Phys.: Condens. Matter **13** (2001) 11473–11484 PII: S0953-8984(01)22893-8

Free-volume microstructure of glycerol and its supercooled liquid-state dynamics

J Bartoš[1,3,4], O Šauša[2], J Krištiak[2], T Blochowicz[1] and E Rössler[1]

[1] Physikalisches Institut, Universität Bayreuth, 95440 Bayreuth, Germany
[2] Institute of Physics of SAS, Dúbravská cesta 9, 842 28 Bratislava, Slovakia

Received 15 March 2001, in final form 19 July 2001
Published 30 November 2001
Online at stacks.iop.org/JPhysCM/13/11473

Abstract

A positron annihilation lifetime spectroscopic (PALS) study was carried out on a typical representative of simple hydrogen-bonded glass formers—glycerol—over a wide temperature region from 100 K up to room temperature. Several crossover temperatures, T_{bi}, were identified in the temperature dependences of the *ortho*-positronium (*o*-Ps) lifetime and the relative *o*-Ps intensity. The onset temperature of free-volume change, 137 K, was compared with the value of 135 ± 3 K obtained from extrapolating thermodynamic data and with the temperatures from relaxation data. In order to determine the influence of the free-volume evolution on the relaxation dynamics above the glass transition temperature T_g, the free-volume fraction from the PALS data was related to the behaviour of the dielectric loss of glycerol. A new relationship between the temperature parameters of the onset of free-volume change and of the high-frequency wing of the dielectric loss is presented. Taking the PALS free-volume data as input for a free-volume model (Doolittle ansatz), it was found that the relaxation times τ_α can be reproduced above the bend temperature $T_{b2} = 241$ K; the latter lies in the vicinity of crossover temperatures reported from mode coupling theory analyses of dynamic data. In the lower-temperature region $T_{b2} > T > T_{b1} \cong T_g$, a contribution from thermally activated mobility has to be included to reproduce the dielectric relaxation time data.

1. Introduction

Glycerol (1, 2, 3-propanetriol) is one of the most systematically studied glass formers. The classical calorimetric studies on both the supercooled liquid and the glassy state of disordered systems started just on this important compound [1a, b]. Later, with the developments of various dynamic techniques such as viscosity [2a–c], ultrasonic [2b, 3a, b] and dielectric relaxation spectroscopy (DRS) [4a–e] light scattering (LS) [5a–d] and neutron

[3] Corresponding author.
[4] On leave from The Polymer Institute of SAS, 842 36 Bratislava, Slovak Republic.

scattering (NS) [6a–c] and NMR [7a–d], glycerol has been repeatedly used as a model system for its good glass formation ability. Glycerol exhibits all the common features of the supercooled liquids, i.e. non-Arrhenius temperature and non-Debye time or frequency behaviours of the primary relaxation [8]. According to the Oldekop–Uhlmann–Angell classification scheme [9a–c] it belongs to the group of the glass-forming liquids of intermediate fragility. The corresponding mean relaxation time–temperature plots are virtually independent of the measuring methods [3b, 7d, 10a–e]. This remarkable behaviour points towards a single relaxation mechanism for various measuring probes [3a], which may be connected with the possibility of forming hydrogen bridges between the molecules and their potential influence on the dynamics in the supercooled liquid state of glycerol [11].

Understanding the phenomenological features of the dynamics in supercooled liquids requires the knowledge of the structural evolution of any glass-forming system on going from the normal fluid liquid through the supercooled liquid state into the rigid glass, where the relaxation time varies over 13–14 decades. Traditionally, x-ray and NS techniques provide important information via the static structure factor. These data however comprise only a projection from 3D space into a one-dimensional structural coordinate and show only more or less smooth continuous temperature dependence of the main–peak position and width, which somehow change at the glass transition temperature, T_g [12a–d]. These studies led to the conclusion that the glassy state behaves like an amorphous solid that keeps the microscopic structure of the liquid.

Positron annihilation lifetime spectroscopy (PALS) is a unique technique for measuring the local variation of density via the *ortho*-positronium (*o*-Ps) probe. Positrons from a ^{22}Na source enter the condensed sample and the lifetime of each single positron is measured. The positron can annihilate as a free positron with an electron in the medium in about $\tau_2 \cong 0.4$ ns or form a metastable bound state called positronium (Ps) together with an electron. If the spins are antiparallel, *para*-positronium (*p*-Ps) is formed, having an intrinsic lifetime $\tau_1 = 0.125$ ns. The *o*-Ps with parallel spins has a lifetime $\tau_{3,0} = 142$ ns in a vacuum. In condensed matter, this lifetime of *o*-Ps is shortened to $\tau_3 \cong 1$–5 ns because the positron can pick off an electron with opposite spin from the surrounding medium and annihilate with it. Thus, *o*-Ps is very sensitive to the presence of various defective regions such as vacancies in crystals or free-volume holes, cavities and voids in disordered systems [13]. The relative intensities of the discussed annihilation channels are I_i, where $i = 1, 2$ and 3. Recent methodological progress enables the extraction from the *o*-Ps data (τ_3 and I_3) of the free-volume characteristics such as the mean free-volume hole sizes [14a–c], R_h, and the free-volume hole fractions [15a, 15b], f_h. Consequently, the availability of these parameters allows us to discuss directly the role of the free-volume factor in the dynamics of supercooled liquids [15b, 16].

The aim of this paper is to present the results of a PALS investigation on glycerol over a wide temperature range and to check the free-volume ansatz by Doolittle describing the relaxation dynamics of the supercooled liquid state as obtained by means of detailed dielectric spectroscopic study [4e, 7d]. Finally, the results of the analysis on glycerol will be compared with those from an analogous study on a typical fragile van der Waals simple glass former, namely *ortho*-terphenyl (OTP) [15b, 16, 17].

2. Experiment

Glycerol as supplied from Aldrich was used in both PALS and dielectric experiments.

The positron annihilation lifetime spectra were obtained by the conventional fast–fast coincidence method using plastic scintilators coupled to Phillips XP 2020 multipliers. The time resolution of prompt spectra was 320 ps. A model-independent instrumental resolution

function was obtained from the decay curve of ^{207}Bi with a single lifetime of 186 ps. In the conventional three-component analysis the PATFIT-88 software package [18] was used.

Temperatures from 100 K up to room temperature, including the glass transition temperature $T_g^{DSC} = 190$ K, were covered.

The details of dielectric measurements and of a phenomenological description of the dielectric loss behaviour of glycerol have been reported in [4e] and [7d].

3. Results

3.1. o-Ps annihilation and free-volume data

Figure 1(*a*) shows both the *o*-Ps annihilation characteristics of glycerol as a function of temperature. The *o*-Ps lifetime, τ_3, exhibits four regions of different temperature behaviour. The transition from one region to the other can be characterized by three crossover temperatures, T_{bi}. The most pronounced change is found at $T_{b1} = 189$ K, which is close to T_g as monitored by dilatometry [19] or calorimetry [1a, b]. Thus, it defines the glass transition temperature as measured by the PALS method, T_g^{PALS}. In addition, the second change is observed in the liquid state at $T_{b2} = 241$ K. This effect at $1.27T_g$ lies in the vicinity of the so-called critical temperature as obtained from recent mode coupling (MCT) analyses [24] of glycerol: $T_{cr}^{LS} = 235$ K [20], $T_{cr}^{DRS} = 249$ K [21], $T_{cr}^{\eta} = 250$ K [22], $T_x^{\eta} = 259$ K [23], $T_{cr}^{DRS} = 262$ K [11] and $T_{cr}^{LS\text{ and }NS} = 262$ K [5d]. Here, the superscripts η, DRS, LS and NS mark the corresponding techniques. On the other hand, a model-independent determination of a crossover temperature was obtained by Stickel *et al* by analysing the temperature dependence of the dielectric relaxation time; this yielded a temperature $T_B = 285$ K [25]. This T_B value is rather close to the third bend temperature at around $T_{b3} = 290$ K, which is characterized by the equality between the mean *o*-Ps lifetime and the characteristic time of the primary α relaxation, τ_α [7d]. The region above T_{b3} indicates a relatively soft matrix characterized by rapid exchange of positions of molecular constituents. Consequently, only below this temperature does the *o*-Ps probe 'feel' relatively rigid surroundings, so that it can be used to characterize the free-volume microstructure of condensed material. A similar temperature dependence of τ_3 has been found also for OTP [17]—see figure 1(b)—as well as a typical polymer glass former: *cis–trans*-1,4-polybutadiene (PBD) [26].

The second *o*-Ps annihilation quantity, the relative intensity, I_3, exhibits three regions of different behaviour (cf figures 1(*a*) and (*b*)). In the glassy state we observe a rather constant value with relatively large scatter. Above T_g^{PALS} two regions with opposite temperature dependences can be found, leading to a minimum at around 260 K. The initial decrease starting just above T_g is replaced by an increase slightly above T_{b2} as obtained from the τ_3–T dependence. A similar behaviour of I_3 can be found in the OTP case—see figure 1(*b*).

The two quantities τ_3 and I_3 have to be converted into free-volume quantities. The mean *o*-Ps lifetime, τ_3, is a measure of the size of the free-volume region, R_h, and both these quantities are related via a semi-empirical quantum mechanical model of *o*-Ps in a spherical hole [14a–c]:

$$\tau_3 = 1/2[1 - R_h/R_0 + (1/2\pi)\sin(2\pi R_h/R_0)]^{-1} \quad (1)$$

where $R_0 = R_h + \Delta R$; $\Delta R = 1.656$ Å is an empirical parameter obtained from fitting PALS data on molecular solids of known hole size such as molecular crystals and zeolites [14b, c]. The mean free-volume hole sizes, V_h, measured for glycerol (see figure 2) are relatively small compared with the van der Waals molecular volume, $V_{mol}^{w} = 86.5$ Å^3, indicating very effective packing of glycerol molecules. At T_g^{PALS} and T_{b2} the mean free-volume hole sizes reach about 23 and 54% of the molecular volume, respectively. At temperature $T \cong 270$ K the mean free-volume hole is comparable to the molecular size. Note that these estimations in glycerol

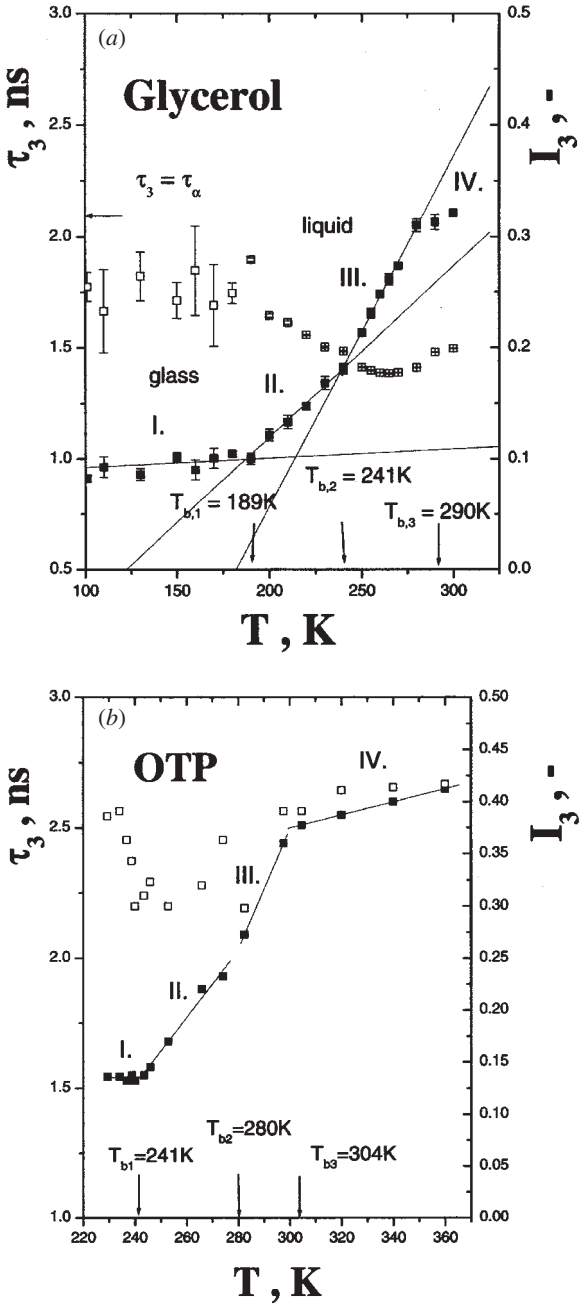

Figure 1. (*a*) Mean *o*-Ps lifetime, τ_3 (■) and *o*-Ps relative intensity, I_3 (□) as a function of temperature for glycerol. (*b*) The same dependences for OTP from the data of [17]. The same symbols as in (*a*).

are comparable to those for OTP [15b], but essentially smaller than those reported for various polymers [26, 27]. This indicates that there is an essential difference in the mean relative free-volume hole sizes between the small-molecular and polymer amorphous systems in identical physical states, (e.g. at $T_{b1} \cong T_g$ or T_{b2}). This may be explained by the connectivity of polymer chains, which does not allow effective filling of the space by the monomer constituents held together by directed bonds.

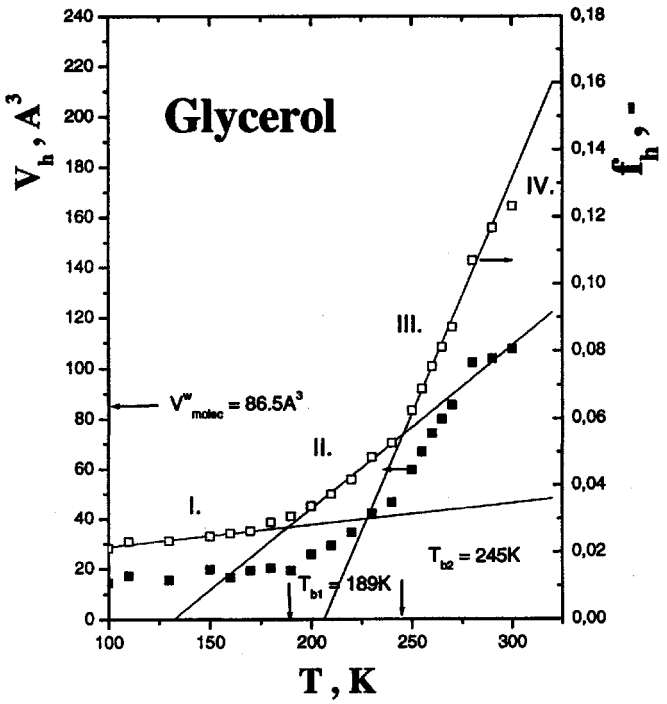

Figure 2. Mean hole volume, V_h (■) and free-volume hole fraction, f_h (□) versus temperature for glycerol as obtained from equations (1)–(4), respectively.

The second free-volume characteristic, i.e. the free-volume hole fraction, f_h, can be obtained from another semi-empirical equation [15a]:

$$f_h(T) = K_{Vh} \cdot V_h(T) \cdot I_3(T) \tag{2}$$

where $I_3(T)$ is the relative o-Ps intensity (a measure of free-volume hole density), $V_h = (4\pi/3)R_h^3$ [13a–c] and K_{Vh} is the proportionality coefficient obtainable from a phenomenological model of volumetric and free-volume hole properties [15b]. This model links the macroscopic volume behaviour from dilatometry to the microscopic free-volume properties from PALS via their respective thermal coefficients in order to quantify the free-volume hole fraction. Starting with a linear dependence of the macroscopic volume V on temperature for a liquid phase above the glass transition temperature, T_g:

$$V(T) = V_i + \beta_V^l(T - T_i) \tag{3}$$

where β_V^l is the liquid-state expansivity and V_i and T_i are the initial (onset) volume or temperature, respectively, at which the free volume $V(T) - V_i$ begins to appear. The free parameters of our model can be determined from both the dilatometric and PALS data and, consequently, their physical meaning can be discussed by comparisons with the relevant thermodynamic and dynamics data. Continuing with the usual definitions of the free-volume fraction $f(T) = V_f(T)/V(T)$ and for its thermal expansion coefficient $\alpha_{f,g} = [1/f(T_g)] \cdot [\Delta f(T)/\Delta T]$, we can arrive at a quadratic equation in T_i,

$$T_i^2 + bT_i + c = 0 \tag{4}$$

where the coefficients contain experimentally accessible quantities only:

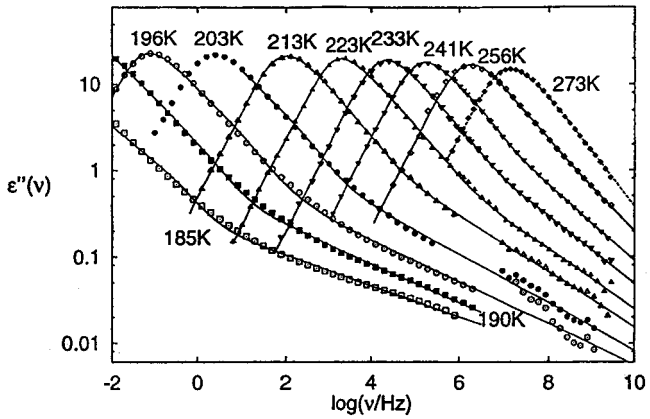

Figure 3. Dielectric loss $\varepsilon''(\nu)$ as a function of frequency, ν, at different temperatures for glycerol from [4e] and [7d].

$$b = -[1 + \alpha^{l}_{V,g}(T + T_g)]/\alpha^{l}_{V,g} \tag{4a}$$

$$c = [(1 + \alpha^{l}_{V,g}T_g)T]/\alpha^{l}_{V,g} + [(1 + \alpha^{l}_{V,g}T)T_g]/[\alpha^{l}_{f,g}(T - T_g)\alpha^{l}_{V,g}] - [(1 + \alpha^{l}_{V,g}T_g)T]/[\alpha_{f,g}(T - T_g)\alpha_{V,g}] \tag{4b}$$

where $\alpha^{l}_{V,g}$ is the thermal expansion coefficient of the macroscopic volume and $\alpha^{l}_{f,g}$ is the thermal expansion coefficient of the free-volume fraction. In the context of the PALS method, the free-volume fraction $f(T)$ can be identified with the free-volume hole fraction $f_h(T)$ through the *o*-Ps annihilation data—equation (2). Then, K_{Vh} can be determined from equations (3) and (4) using V–T liquid-state data.

Thus, in the case of glycerol, by using the input data, i.e. $\alpha_{V,g} = 4.8 \times 10^{-4}$ K^{-1} [19], $\alpha_{fh,g} = 1.78 \times 10^{-2}$ K^{-1}, $T_g = 190$ K and the higher boundary temperature of region II, $T = 240$ K, we obtain $T_i = 137$ K and the corresponding packing coefficient $p_i = V^{w}_{mol}/V_i = 0.75$. The temperature T_i is in good agreement with the Kauzmann temperature of glycerol [28a], at which the extrapolated entropy of the supercooled liquid reaches that of the corresponding crystal $T_K = 135 +/- 3$ K [28b–d] as determined from the data of the original calometric results [1b]. In addition, T_i is quite consistent with the Vogel temperatures, T_0, at which the relaxation time diverges, as found from numerous fittings to dynamic data by the Vogel–Fulcher–Tammann–Hesse (VFTH) equation [2a, 3b, c, 4a–d, 5c, 10a–e, 11]. This observation is similar to that for OTP [15b] with one exception. In the case of OTP, the identification of T_0 is rather sensitive to the temperature interval used in the VFTH equation fit. The second free parameter of the model, p_i, obtained for glycerol lies in the vicinity of that of the closest regular packing of hard spheres, 0.74. Again, similar results are found for the OTP case [15b].

Having determined both free parameters of the phenomenological volumetric–free-volume model, we can fix the calibration coefficient K_{Vh} to be 5.14×10^{-3} Å^{-3} and the resulting effective free-volume hole fraction is depicted in figure 2. These values will be utilized in analysis of the role of the free-volume hole factor in the supercooled liquid dynamics. Note that the free-volume hole fraction ranges from about 2% in the glassy state up to 12% at around T_{b3}.

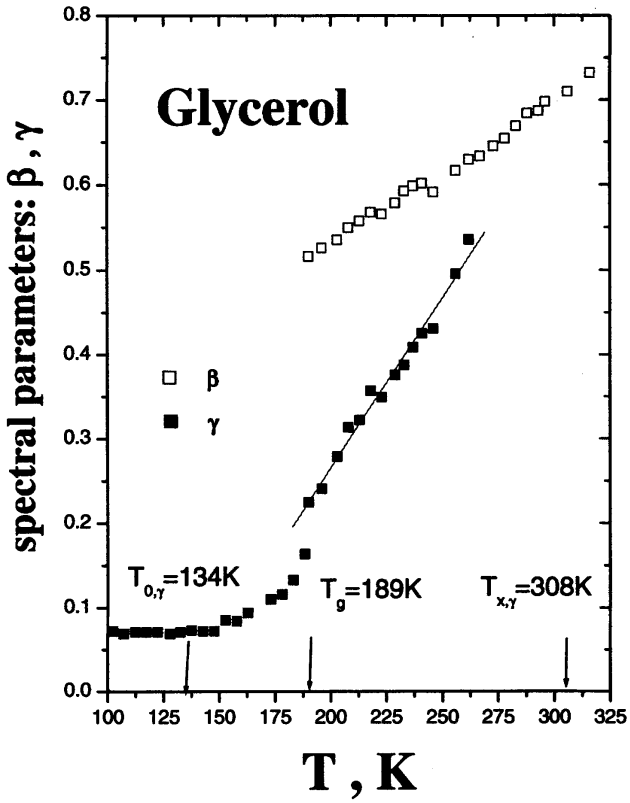

Figure 4. Spectral parameters β and γ of the imaginary part of the dielectric susceptibility as a function of temperature for glycerol from [4e] and [7d].

3.2. Dielectric relaxation data

The results of the detailed DRS studies [4e,7d] on glycerol over wide temperature and frequency ranges are compiled in figure 3, where the dielectric relaxation data in terms of log ε'' versus log ν are presented. Here, ε'' marks the imaginary part of the dielectric sucsceptibility at measuring frequency ν as a measure of the dipole reorientational mobility. The data include not only the primary α relaxation peak region characterized by the $\varepsilon''(\nu) \propto \nu^{-\beta}$ power law at $\nu > \nu_{\text{peak}}$, but also its high-frequency wing at $\nu \gg \nu_{\text{peak}}$, for which $\varepsilon''(\nu) \propto \nu^{-\gamma}$, with $\beta > \gamma$. The relaxation peak can be interpolated by a Cole–Davidson (CD) function [4a, b], while both the first and second power-law regimes can be quantitatively described by a novel generalized Cole–Davidson (G-CD) function [4e, 7d]. Figure 4 represents the temperature dependences of both exponents, β and γ, from 100 K up to 320 K. The β exponent depends slightly on temperature, indicating that the frequency superposition principle holds in first approximation for the frequency region around the relaxation peak. On the other hand, the γ exponent exhibits stronger temperature dependence. At high temperatures β and γ become similar, which may indicate that the wing disappears at highest temperatures. Well below T_{g} the exponent appears to be frozen in at a very low value. Similar results have been reported in the literature [29a–c]. In addition, the mean relaxation time of the primary α process, τ_α, as a function of temperature is presented in figure 5. All these fitting parameters of the lineshape analysis are to be interpreted in the context of the PALS results. This will be the subject of the following section relating the structural and dynamical information.

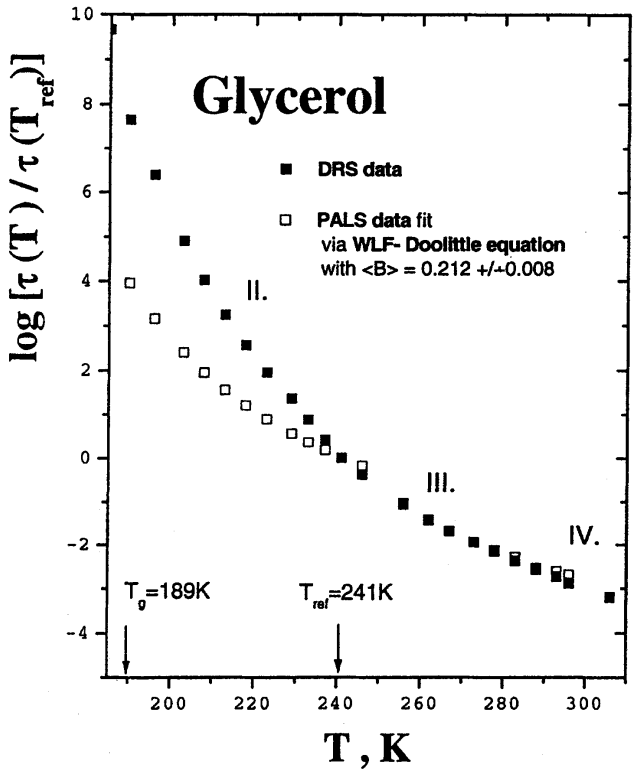

Figure 5. Relationship between the α relaxation time, τ_α, from dielectric spectroscopy and the free-volume hole fraction, f_h, from the PALS method for glycerol in terms of the WLF-Doolittle-type equation (5) with $T_{ref} = 241$ K.

4. Discussion

4.1. Relationships between o-Ps annihilation, free-volume hole and relaxation data

Having compiled PALS and DRS data on the same sample glycerol offers a unique opportunity to relate structural and dynamic properties. On cooling, the change of slope in the dependence of τ_3 on T at around 240 K in figure 1(a) may reflect the impact of the onset of certain frustrational constraints, such as clusters or even microcrystals on the free-volume hole contraction still in the liquid state above T_g. This may lead to the change in the motional state of supercooled liquid and to the approximate identity of T_{b2} with the crossover temperatures T_{cr} determined from mode-coupling theory (MCT) analyses of a series of dynamic quantities. Thus, our experimental finding of the different *o*-Ps lifetime expansivities above and below the temperature $T_{b2} \approx T_{cr}$ suggests the structural origin of dynamic change in the supercooled liquid above T_g.

The initial decrease in I_3 just above T_g in figure 1(a) suggests the existence of some relative rapid motion because a fraction of the free-volume sites for *o*-Ps localization can be eliminated due to some mobility on a timescale of up to nanoseconds—the blocking hypothesis [30]. Indeed, the dielectric data on glycerol (see figure 3) reveal the presence of such a motion, which is manifested by the high-frequency wing of the relaxation peak of the primary α-process close to T_g [4c,31]. With increasing temperature and the accompanying macroscopic volume expansion the blocking effect of the localized rapid mobility is reduced and, consequently, I_3 begins to increase. This finding is consistent with the above-mentioned releasing of restricting constraints on the expansion of free-volume holes during heating of the sample beyond $T \cong 240$ K.

Phenomenologically, the high-frequency motion is characterized by the γ exponent (see figure 4). Linear extrapolations of $\gamma(T)$ in the liquid, i.e. above T_g, provide two interesting limiting cases, which can be related to the PALS results. The low-temperature extrapolation to $\gamma = 0$ gives $T_{0,\gamma} = 134$ K, which agrees with the above-mentioned initial temperature of the free-volume change T_i, with the Vogel temperatures T_0 from various dynamic quantities as well as the Kauzmann temperature T_K. Although it is not clear whether the high-frequency wing strictly belongs to the primary α relaxation, or may be regarded rather as some sort of secondary relaxation [32a, b], this coincidence seems to suggest that many dynamic properties of supercooled liquid glycerol have a common origin and supports the idea that the wing might at least be a precursor of the α relaxation in glycerol.

On the other hand, the high-temperature extrapolation to the case $\gamma = \beta$ gives $T_{x,\gamma} = 308$ K, which is in the vicinity of $T_{b3} = 290$ K from PALS and apparently consistent with the fluid character of liquid. However, this extrapolation must be considered as tentative only, because the high-frequency wing feature apparently disappears already at around 265 K, consistent with our findings that $I_3(T)$ reverses its trend with temperature (from decreasing to increasing) and that the mean free-volume hole size becomes comparable to the molecular volume.

Summing up these findings we can suggest that the high-frequency wing might be some type of localized 'in-cage' motion which precedes the large-scale 'out-cage' primary α relaxation and is reflected by the PALS data.

After having established these mutual relationships between the free-volume microstructure and the primary α relaxation, including its high-frequency part, we can analyse the role of the free-volume factor in the dielectric relaxation dynamics directly. Figures 5 and 6 show the results of the analysis of further fitting quantities from the detailed DRS study, i.e. the mean α relaxation time, τ_α, in terms of free-volume hole fraction $f_h(T)$ from figure 2.

The WLF-Doolittle-type equation [33a, b],

$$\log a_\tau(T) \equiv \log \tau(T)/\tau(T_{ref}) = \langle B \rangle [1/f_h(T) - 1/f_h(T_{ref})] \tag{5}$$

where T_{ref} is an appropriately chosen reference temperature and $\langle B \rangle = B/2.303$ is a fitting parameter, works quite well in region III—see figure 5. According to the Cohen–Turnbull statistical–mechanical interpretation [34] of the Doolittle equation, the B-coefficient is a measure of the critical free volume necessary for the movement of a kinetic unit. Thus, the $\langle B \rangle$ fitting parameter coefficient can be considered as a measure of the extent of the cooperative region of supercooled liquid responsible for free-volume redistribution which leads to the formation of a critical free-volume hole in the immediate neigbourhood of the moving entity participating in the primary relaxation. Outside region III we observe deviations from equation (5). Above 290 K the deviation is due to the equality between τ_3 and τ_α and, hence, the intrinsic limitation of the PALS method. It is interesting to note that the onset of this departure agrees with the crossover temperature at 285 K for the crossing from the VFTH (or Doolittle) equation to the Arrhenius one [25].

At lower temperatures, below $T_{ref} = T_{b2} = 240$ K, the character of the deviation suggests some additional factor which contributes to the primary relaxation process. The two basic factors controlling the motion in condensed matter, i.e. the free volume and thermal activation, may be combined to yield a single equation. This was introduced by formulating the WLF-Doolittle–Macedo–Litovitz-type equation [35]:

$$\log a_\tau(T) = \langle B \rangle [1/f_h(T) - 1/f_h(T_{ref})] + (E_{act}/2.303R)[1/T - 1/T_{ref}]. \tag{6}$$

Here, E_{act} is the activation energy. This approach can be used in the analysis of the difference between the measured $\log a(T)$ dependence and the free-volume contribution obtained from PALS. Figure 6 shows that this additional factor indeed obeys the Arrhenius law with

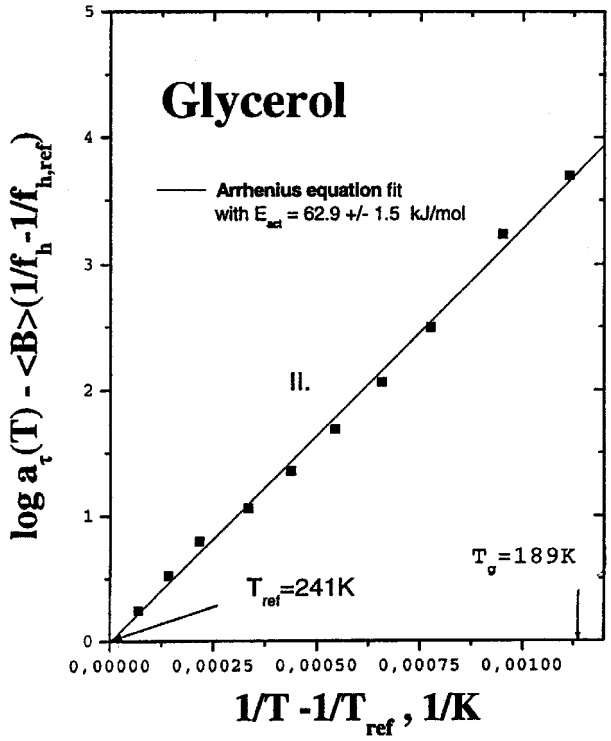

Figure 6. Test of the WLF-Macedo–Litovitz-type equation (equation (6)) for $T < T_{\rm ref}$ for glycerol in terms of the difference between the measured shift factor $a_\tau(T)$ and the free-volume term $\langle B\rangle[1/f_{\rm h}(T) - 1/f_{\rm h}(T)]$ calculated using free-volume hole fractions for $T < T_{\rm ref}$.

$E_{\rm act} = 63 \pm 2$ kJ mol^{-1}. This value is about three times the typical cohesive energy of the hydrogen-bond bridge (≈20 kJ mol^{-1}) [36a–c].

We note that the change from the free-volume-dominated regime to that controlled by both the free volume and the thermal activation at around 240 K does not necessarily indicate the onset of hydrogen bonding among molecules, because they can be formed already above $T_{\rm b2}$, as in simple alcohols [37]. It might mean a qualitative change in the impact of hydrogen bonding of molecules on the cooperative α relaxation. This statement seems to be consistent with the results of the analysis of the density data of glycerol in terms of the simple cluster model [38a, b]: on cooling the volume fraction of clusters of the bonded molecules increases slightly from room temperature down to 233 K, where it achieves 10%, and grows further more steeply up to a level of 30% at $T_{\rm g}$, where an infinite percolating cluster of strongly bonded molecules should be formed [38a, b].

Finally, our finding of a transition from the free-volume-controlled regime above $T_{\rm b2}$ to the combined free-volume and thermal activation one at lower temperatures seems to resemble the potential energy landscape concept [39a–d] postulating the growing role of thermal-activated dynamics with decreasing temperature. However, in contrast to the original landscape postulate, the sub-$T_{\rm b2}$ dynamics of glycerol is dominated by a common action of both the free-volume and the thermal activation factors and not by the activation energy term alone.

4.2. Comparison of intermediate and fragile simple glassformers

In this section, we compare the two low-molecular-weight glass formers analysed so far from the point of view of free-volume theory: glycerol as a liquid with an intermediate fragility

$m_g = 53$ [40] and OTP [15b, 17] with a high fragility ($m_g = 81$) [40]. In spite of their different chemical structure (H-bridge bonded versus van der Waals system) both molecular glass formers exhibit universal behaviour in the *o*-Ps data—see figures 1(a) and (b): (i) the τ_3–T dependence bends at $1.27T_g$ or $1.17T_g$, respectively and (ii) the I_3–T dependence shows similar behaviour, consisting in a decrease (minimum) just above the particular T_g in the vicinity of the bend temperature. On the other hand, the main difference is the fact that the dynamics of OTP can be reproduced over the whole liquid range [15b] by taking the effective PALS free-volume hole fraction, while for glycerol the structural relaxation is controlled by this factor only above T_{b2}; below T_{b2} an activation-energy term has to be included. This comparison implies that the H-bond bridges alone are not responsible for the presence of the change of slope in the τ_3–T dependence, although they influence essentially the fragility of glycerol with respect to OTP as well as the polymer glass former PBD [26]. The open question remains what causes the characteristic changes in the temperature dependence of the PALS parameters in all the types of glass former in the supercooled liquid state above T_g. Evidently, a deeper understanding of these phenomena requires the application of an interdisciplinary approach combining PALS with various dynamic techniques on further suitable chosen model systems.

Acknowledgments

JB wishes to thank the Alexander von Humboldt-Foundation, Germany, for the fellowship to complete this work and, together with JK, the VEGA Agency, Slovakia, for support by grants no 2/7067/20 and no 2/1123/21, respectively. The first author thanks M Vogel and Ch Tschirwitz for helpful discussions and S Adichtschev for technical assistance.

References

[1a] Simon F 1922 *Ann. Phys., Lpz.* **68** 241
[1b] Gibson G E and Giaugue W F 1923 *J. Am. Chem. Soc.* **45** 93
[2a] Tammann G and Hesse W 1926 *Z. Anorg. Allg. Chem.* **156** 245
[2b] Piccirelli R and Litovitz T 1957 *J. Acoust. Soc. Am.* **29** 1009
[2c] Herbst C A, Cook R L and King H E 1993 *Nature* **361** 518
[3a] Jeong Y H, Nagel S and Bhattacharya S 1986 *Phys. Rev.* A **34** 602
[3b] Jeong Y H 1987 *Phys. Rev.* A **36** 766
[4a] Davidson D W and Cole R H 1950 *J. Chem. Phys.* **18** 1417
Davidson D W and Cole R H 1951 *J. Chem. Phys.* **19** 1484
[4b] Dixon P K, Wu L, Nagel S R, Williams B D and Carini J P 1990 *Phys. Rev. Lett.* **65** 1108
[4c] Menon N, O'Brien K P, Dixon P, Wu L, Nagel S R, Williams B D and Carini J P 1992 *J. Non-Cryst. Solids* **141** 61
[4d] Lunkenheimer P, Pimenov A, Schiener B, Böhmer R and Loidl A 1996 *Europhys. Lett.* **33** 611
[4e] Kudlik A, Benkhof S, Blochowicz T, Tschirwitz T and Rössler E 1999 *J. Mol. Liq.* **479** 201
[5a] Demoulin C, Montrose C J and Ostrovsky N 1974 *Phys. Rev.* **9** 1740
[5b] Posch H A, Dardy H D and Litovitz T A 1977 *Ber. Bunsenges. Phys. Chem.* **81** 744
[5c] Dux H and Dorfmüller T 1979 *Chem. Phys.* **40** 219
[5d] Wuttke J, Hernandez J, Li G, Cummins H Z, Fujara F, Petry W and Sillescu H 1994 *Phys. Rev. Lett.* **72** 3052
[6a] Fujara F, Petry W, Diehl R M, Schnauss W and Sillescu H 1991 *Europhys. Lett.* **14** 563
[6b] Wuttke J, Petry W, Coddens G and Fujara F 1995 *Phys. Rev.* E **52** 4026
[6c] Wuttke J, Petry W and Pouget S 1996 *J. Chem. Phys.* **105** 5177
[7a] Bloembergen N, Purcell E M and Pound R V 1948 *Phys. Rev.* **73** 679
[7b] Diehl R H, Fujara F and Sillescu H 1990 *Europhys. Lett.* **13** 257
[7c] Böhmer R and Hinze G 1998 *J. Chem. Phys.* **109** 241
[7d] Blochowicz T, Kudlik A, Benkhof S, Senker J, Rössler E and Hinze G 1999 *J. Chem. Phys.* **110** 12 011
[8] Ediger M D, Angell C A and Nagel S R 1996 *J. Phys. Chem.* **100** 13 200
[9a] Angell A C 1985 *Relaxation of Complex Systems* (Springfield, IL: National Technical Information Service)
[9b] Laughlin W and Uhlmann D 1972 *J. Phys. Chem.* **76** 2317

[9c] Oldekop W 1957 *Glastech. Ber.* **30** 8
[10a] Birge N O, Jeong Y H and Nagel S R 1986 *Ann. NY Acad. Sci.* **484** 101
[10b] Lunkenheimer P, Schneider U, Brand R and Loidl A 2000 *Contemp. Phys.* **41** 15
[10c] Wuttke J 2000 *Advances in Solid State Physics* (Braunschweig: Vieweg)
[11] Lunkenheimer P, Pimenov A, Dressel M,Goncharov Yu G, Böhmer R and Loidl A 1996 *Phys. Rev. Lett.* **77** 318
[12a] Busse L and Nagel S R 1981 *Phys. Rev. Lett.* **47** 1848
[12b] Soltwisch M and Steffan B 1981 *Z. Naturf.* A **36** 1045
[12c] Champaney D C, Joarder R N and Dore J C 1986 *Mol. Phys.* **58** 337
[12d] Leheny R L, Menon N, Nagel S R, Price D L, Suzuy K and Thiyagarajan P 1996 *J. Chem. Phys.* **105** 7783
[13] Dupasquier A and Mills A P Jr (eds) 1995 *Positron Spectroscopy of Solids* (Amsterdam: Ohmsha)
[14a] Tao S J 1972 *J. Chem. Phys.* **56** 5499
[14b] Eldrup M, Lightbody D and Sherwood J N 1981 *Chem. Phys.* **63** 51
[14c] Nakanishi H and Jean Y C 1988 *Positron and Positronium Chemistry* (Amsterdam: Elsevier) p 159
[15a] Kobayashi Y, Zheng W, Meyer E F, McGervey J D, Jamieson A M and Simha R 1989 *Macromolecules* **22** 2302
[15b] Bartoš J and Krištiak J 2000 *J. Phys. Chem.* B **104** 5666
[16] Bartoš J and Krištiak J 1999 *J. Phys.: Condens. Matter* **11** A371
[17] Malhotra B D and Pethrick R A 1982 *J. Chem. Phys. Faraday Trans.* **78** 297
[18] Kirkegaard P, Eldrup M, Mogensen O E and Pedersen N J 1989 *Comput. Phys. Commun.* **23** 307
[19] Kovacs A 1963 *Adv. Polym. Sci.* **3** 394
[20] Franosch T, Götze W, Mayr R and Singh A P 1997 *Phys. Rev.* E **55** 3183
[21] Schönhals A, Kremer F, Hoffman A and Fischer E W 1993 *Phys. Rev. Lett.* **70** 3459
[22] Richert R and Bässler H 1990 *J. Phys.: Condens. Matter* **2** 2273
[23] Rössler E, Hess K U and Novikov V N 1998 *J. Non-Cryst. Solids* **223** 207
[24] Götze W and Sjögren L 1992 *Rep. Prog. Phys.* **55** 241
[25] Stickel F, Fischer E W, Schönhals A and Kremer F 1994 *Phys. Rev. Lett.* **73** 2936
[26] Bartoš J, Šauša O, Bandžuch P, Zrubcová J and Krištiak J 2000 *Proc. 3rd Int. Conf. on Mechanics of Time Dependent Materials (Erlangen)* p 112
[27] Bartoš J 1996 *Colloid. Polym. Sci.* **274** 14
[28a] Kauzmann W 1948 *Chem. Rev.* **43** 219
[28b] Angell C A and Rao K J 1972 *J. Chem. Phys.* **57** 470
[28c] Angell C A and Smith D L 1982 *J. Phys. Chem.* **86** 3845
[28d] Angell C A 1997 *J. Res. Natl Inst. Stand. Technol.* **102** 171
[29a] Menon N and Nagel S R 1995 *Phys. Rev. Lett.* **74** 1230
[29b] Leheny R L and Nagel S R 1997 *Europhys. Lett.* **39** 447
[29c] Leheny R L, Nagel S R 1998 *J. Non-Cryst. Solids* **235–7** 278
[30] West D H D, McBrierty V J and Delaney C F 1975 *Appl. Phys.* **7** 171
[31] Schneider U, Lunkenheimer P, Brand R and Loidl A 1998 *J. Non-Cryst. Solids* **235–7** 173
[32a] Leon C A and Ngai K L 1999 *J. Phys. Chem.* B **103** 4045
[32b] Schneider U, Brand R, Lunkenheimer P and Loidl A 2000 *Phys. Rev. Lett.* **84** 5560
[33a] Doolittle A K 1951 *J. Appl. Phys.* **22** 1471
[33b] Williams M L, Landel R F and Ferry J D 1955 *J. Am. Chem. Soc.* **77** 3701
[34] Cohen M H and Turnbull D 1959 *J. Chem. Phys.* **31** 1164
[35] Macedo P B and Litovitz T A 1965 *J. Chem. Phys.* **42** 245
[36a] Pimentel G C and McClellan A L 1960 *The Hydrogen Bond* (San Francisco: Freeman)
[36b] Vinogradov S N and Linnell R H 1971 *Hydrogen Bonding* (New York: Van Nostrand-Reinhold)
[36c] Schuster P 1976 *The Hydrogen Bond I Theory* (Amsterdam: North-Holland)
[37] Luck W A and Ditter W 1968 *Ber. Bunsenges. Phys. Chem.* **72** 365
[38a] Malomuzh N P and Pelishenko S B 1991 *Phys. Lett.* A **154** 269
[38b] Lishchuk S V and Malomuzh N P 1997 *J. Chem. Phys.* **160** 6160
[39a] Goldstein M 1969 *J. Chem. Phys.* **51** 3728
[39b] Stillinger F H 1995 *Science* **267** 1935
[39c] Angell C A 1998 *Nature* **393** 521
[39d] Schroder T B, Sastry S, Dyre J C and Glotzer S C 2000 *J. Chem. Phys.* **112** 9854
[40] Böhmer R, Ngai K L, Angell C A and Plazek D J 1993 *J. Chem. Phys.* **99** 5201